Letters

Reconfigurable Battery Charger With a Wide Voltage Range for Universal Electric Vehicle Charging Applications

Harish Karneddi, *Student Member, IEEE*, and Deepak Ronanki, *Senior Member, IEEE*

***Abstract*—The extant battery chargers are incompatible with the current and next-generation electric vehicles (EVs) due to disparities in their battery pack voltages. This letter introduces a new reconfigurable battery charger to charge the existing and next-generation EV battery packs with the same power rating, only one relay and a filter capacitor branch, unlike existing solutions where many passive and active components are utilized for reconfiguration. Also, the proposed configuration avoids a large grid-side filter requirement due to boost–buck configuration. Furthermore, a mode switching-based control scheme is proposed to operate the charger in an extremely wide voltage range with the possibility of intermediate battery voltage charging options. The MATLAB simulations and experimental studies on a 1.3-kW silicon carbide MOSFET-based laboratory prototype reveal the feasibility of the proposed reconfigurable charger for low-, medium-, and high-voltage EV battery pack charging.**

***Index Terms*—AC–DC power converters, battery chargers, electric vehicles (EVs), power converters.**

I. Introduction

GENERALLY, electric vehicles (EVs) are charged by wired and wireless chargers. However, wired chargers are more popular owing to their greater efficiency, ease of design, and control. With the rise in EV growth, it is worth noting that their nominal battery voltages are not always the same [1]. Existing EVs, such as Nissan Leaf S, Tesla Model X, FIAT new 500e, and Mercedes-Benz EQA, have battery voltages ranging from 250 to 450 V. Therefore, wide-voltage battery chargers (250–450 V) are developed to charge these battery packs [2]. Alternatively, next-generation EVs, such as Rapide E, Lucid Air, Porsche Taycan, Hyundai IONIQ, and KIA EV6, come with high-voltage (HV) battery pack voltages ranging from 600 to 800 V, being advantageous in terms of achieving substantial EV weight savings and a significant decrease in charging time [3], [4]. However, charging these batteries with existing chargers degrades the efficiency due to operating at twice the nominal voltage. On the other hand, HV chargers are inadequate for low-voltage (LV) and medium-voltage (MV) battery pack charging. Therefore, the challenge for the battery chargers is obvious: to offer charging services to various EVs, which will necessitate the operation of power electronic circuits over an extremely wide range of battery voltages.

Over the past years, several charger configurations and solutions have been presented to charge the 400 and 800-V EV battery packs [5], [6], [7], [8], [9], [10]. A reconfigurable solution is proposed to charge an 800-V battery pack from a 400-V charger by reconfiguring the battery pack and battery management system (BMS) [5]. However, this charger configuration is expensive, does not reduce the charging cord size, and is complex. On the other hand, reconfigurable battery chargers are proposed to replenish the energy into 400- and 800-V batteries from a single charging unit [6], [7], [8], [9]. Moreover, these topologies are limited to only charging 400- and 800-V EV battery packs. Also, there is no possibility of charging an intermediate battery pack voltage level (e.g., 600-V KIA EV [1]). A reconfigurable dc–dc converter is proposed to charge intermediate battery pack voltages ranging from 250 to 1000 V [10]. Nevertheless, these chargers demand additional auxiliary devices, such as high-frequency (HF) tap-changing transformers (TFs), battery selection circuits, HF three-winding TFs, front-end diode bridge rectifiers, active switches, and cascaded secondary rectifiers. In addition, these chargers operate with a 640–840 V dc input supply, which makes this configuration confined to offboard charging applications. Furthermore, it degrades the power density, device utilization, and incurs higher costs. To the best of the authors' knowledge, no studies are related to a battery charger that provides a wide voltage range to charge the battery pack voltages range from 120 to 900 V.

This letter proposes a new reconfigurable battery charger with a wide output voltage range without introducing many additional passive and active components. Unlike existing chargers, the proposed charger is a boost–buck configured topology at the grid side, which avoids/minimizes the input filter requirement. A mode switching-based control with a seamless transition is proposed to operate the charger in an extremely wide voltage range (120–900 V) while maintaining the charging standards and grid code requirements. An experimental prototype of a 1.3-kW charger is implemented to validate the proof-of-concept. Finally, the effectiveness of the proposed charger is evaluated through simulation and experimental studies and compared with the existing chargers.

Manuscript received 24 April 2023; revised 22 May 2023; accepted 19 June 2023. Date of publication 28 June 2023; date of current version 28 July 2023. This work was supported in part by the Science and Engineering Research Board (SERB), the Department of Science and Technology (DST), Government of India under Startup Research Grant (SRG) SRG/2021/000184. *(Corresponding author: Deepak Ronanki.)*

The authors are with the Department of Engineering Design, Indian Institute of Technology Madras, Chennai 600036, India (e-mail: ed20d016@smail.iitm.ac.in; dronanki@ieee.org).

Color versions of one or more figures in this article are available at https://doi.org/10.1109/TPEL.2023.3289394.

Digital Object Identifier 10.1109/TPEL.2023.3289394

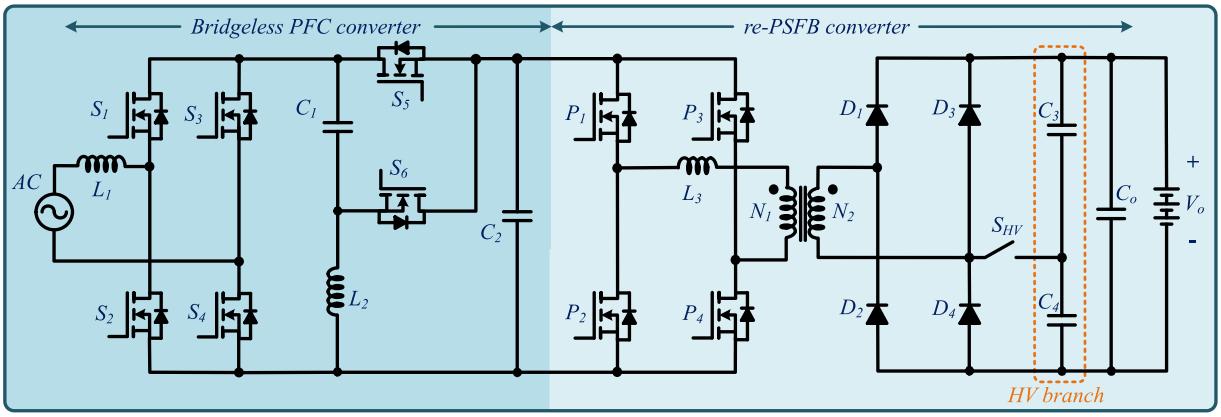

Fig. 1. Proposed wide voltage-range reconfigurable isolated battery charger for universal EV charging.

II. Proposed Reconfigurable Battery Charger

A reconfigurable battery charger depicted in Fig. 1 is proposed for charging LV–MV–HV (universal) battery packs with the same power rating. This charger features a two-stage isolated topology derived from a wide voltage range bridgeless boost–buck power factor correction (PFC) converter and a reconfigurable phase-shifted full bridge (re-PSFB) converter. The boost operation is carried out by switches S_1–S_4, inductor L_1, and the buck operation is fulfilled with S_5, S_6, capacitor C_1, and L_2. In the boost mode, buck switches remain idle, and the buck arm assists the dc-link filter. Whereas in the buck mode, boost switches remain idle. Moreover, the boost inductor L_1 and C_1 form a low-pass filter and attenuate the higher order ripple in input current. Therefore, the values of L_1 and C_1 were chosen not to affect the fundamental current.

The reconfigurable dc–dc converter has a similar configuration as a conventional PSFB on the primary side. However, an HV capacitor branch (C_3 and C_4) and a switch S_{HV} are incorporated on the secondary side along with the diode bridge rectifier. The efficiency of traditional PSFB converters is higher for low phase shifts and drastic decreases as phase shift increases [11]. Therefore, the proposed charger's front-end PFC converter operates such that re-PSFB always operates with a minimal phase shift irrespective of the battery pack voltages. As a result, the re-PSFB converter operates as an isolated dc–dc converter with unity gain for LV and MV EV charging ($V_o < 450$ V). Furthermore, the HV capacitor branch assists the output filter and significantly reduces output voltage ripple, which can be given as follows:

$$\Delta V_o = \frac{d_2(t)|V_{\text{max}}\sin(\omega t)|\,[1-2d_3(t)]}{16(1-d_1(t))f_{\text{sw}}^2 L_3\left(C_o + \frac{C_3C_4}{C_3+C_4}\right)} \tag{1}$$

where ΔV_o, V_{max}, $\omega = 2\pi f_{\text{in}}$, f_{sw}, $d_1(t)$, $d_2(t)$, and $d_3(t)$ are the output ripple voltage, maximum input voltage, angular input frequency, switching frequency, duty cycles of boost and buck modes, and re-PSFB converter duty cycle, respectively. On the other hand, for the HV powertrain charging ($V_o > 450$ V), the switch S_{HV} is ON. Subsequently, the re-PSFB converter operates with a gain of approximately 2. The comprehensive operating mode selection of the proposed charger with respect to input and battery pack voltages is shown in Fig. 2.

The proposed charger's front-end converter and a re-PSFB converter are controlled with two distinct controllers, as shown

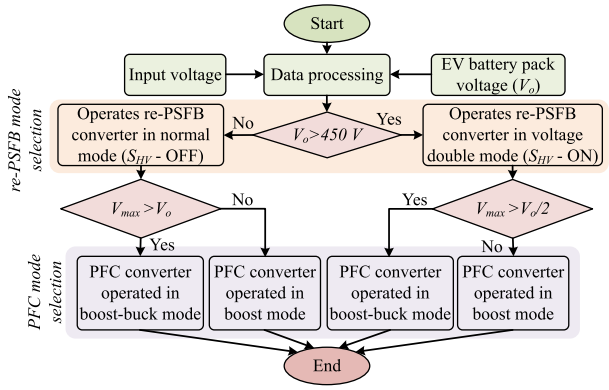

Fig. 2. Operating mode selection strategy flowchart of the proposed reconfigurable battery charger.

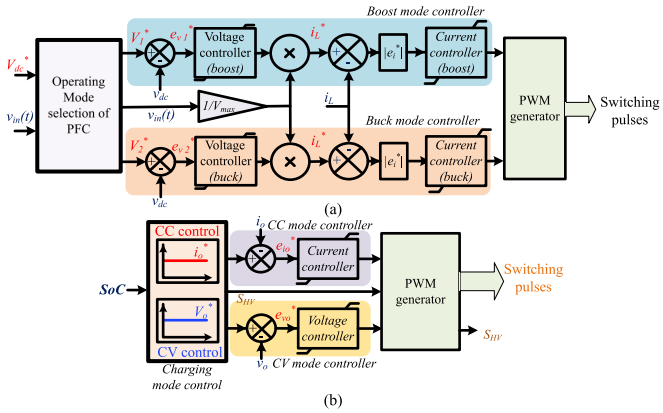

Fig. 3. Control architectures of the proposed battery charger. (a) Front-end converter controller. (b) re-PSFB converter controller.

in Fig. 3(a) and (b). The PFC converter involves two dual-loop controllers to accomplish the boost and buck operations. The inner loop is a current control loop, whereas the outer loop is a dc-link voltage control loop. The inner loop is designed with a significantly higher bandwidth to preserve the sinusoidal current in phase with the input voltage. In contrast, it should be less than the switching frequency to attenuate the ripple in the error current. The dc-link voltage comprises a 2nd harmonic ripple,

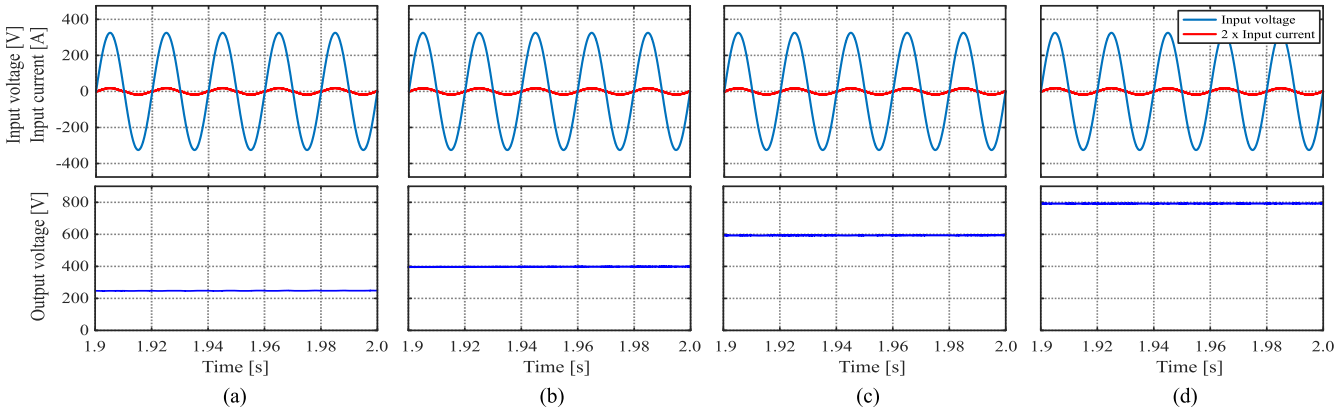

Fig. 4. Performance of the proposed reconfigurable battery charger with a 230 V, 50 Hz input supply. (a) 250-V charging. (b) 400-V charging. (c) 600-V charging. (d) 800 V-charging.

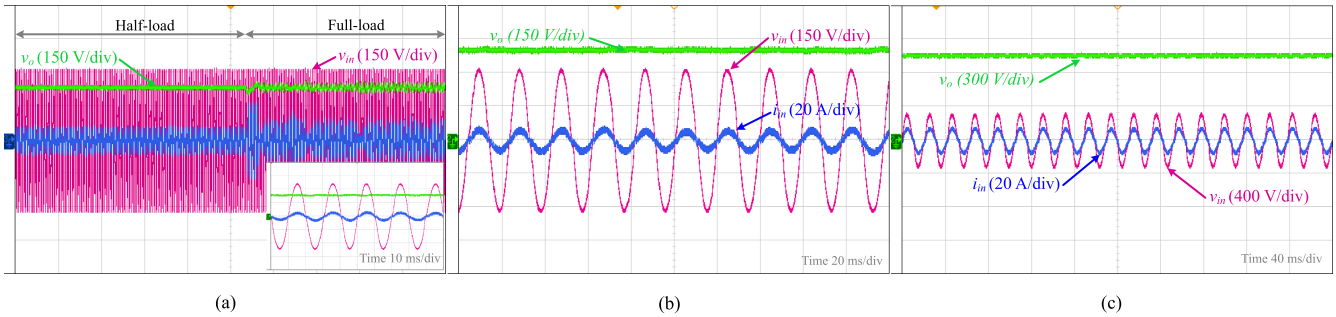

Fig. 5. Test results of the proposed battery charger: 230 V, 50 Hz input. (a) Dynamic performance of 250-V charging (step change in load). (b) Steady-state performance of 400-V charging. (c) Steady-state performance of 800-V charging.

which appears in the error voltage as given follows:

$$e_v{}^* = \frac{V_{\max} I_{\max}}{4 V_o \omega C_2} \sin(2\omega t) \tag{2}$$

where $I_{\max}$ is the maximum input current. Therefore, the outer voltage loop is designed with a much smaller bandwidth to attenuate the 2nd harmonic error voltage. Similarly, the re-PSFB converter controller shown in Fig. 3(b) maintains the desired current/voltage to charge the battery with a constant current–constant voltage (CC–CV) charging technique and S_{HV} is operated once in a charging period based on the battery pack voltage. The gain coefficients of these controllers are designed using the frequency response analysis of derived charger's transfer functions.

III. Results and Discussion

A 1.3-kW charger is designed to evaluate the proposed reconfigurable battery charger and its controller. The design specifications and required component ratings are listed in Table I. The charger's controllers are realized with linear proportional-integral controllers. The front-end converter current controllers are designed with a 20-kHz bandwidth, whereas the voltage controllers are designed with 12 Hz. The CC–CV charging technique has been adopted for battery charging [12], [13]. The simulations are performed with a 230-V, 50-Hz input supply, and the battery is realized with an equivalent resistive load. The charger is simulated for charging 250, 400, 600, and 800 V battery pack voltages, and the corresponding results are shown in Fig. 4.

TABLE I
Specifications and Component Values of the Charger

Specifications of the converter		Component values	
Parameters	Rating	Component	Rating
Input voltage	85–265 V	L_1	0.55 mH
Input frequency	50/60 Hz ± 1%	C_1	44 μF
Power rating	1.3 kW	L_2	0.43 mH
Current ripple	20%	C_2	0.94 mF
Switching frequency	50 kHz	L_3	10 μH
Voltage ripple	10%	C_3	0.47 mF
Holding time (t_{hold})	20 ms	C_4	0.47 mF
HFTF transformation ratio	1.02	C_o	0.94 mF

A 1.3-kW laboratory prototype is designed with CREE C2M0040120D silicon carbide (SiC) MOSFETs, TDK electronics-B82727E6503A040 inductors, CDE-381LR471M450A052 capacitors, and MSC50DC120HJ SiC diode bridge rectifier. A 1-ϕ autotransformer is used as input power supply, and the battery is realized with an equivalent resistive load. Finally, the controllers are implemented on a WAVECT WCU-300 real-time controller, and a relay is used as an S_{HV}. The proposed charger's test results are depicted in Fig. 5. From the simulation and experimental studies, it is noticed that the proposed charger and the designed controller maintained a sinusoidal current with approximately unity power factor (UPF) while preserving the required output voltage. In addition, the mode selection-based controller quickly brings the charger into a steady state of operation under load variations.

One of the main concerns with wide voltage range chargers is that the device amperage will vary with the battery pack voltages. Therefore, detailed studies are made to assess the

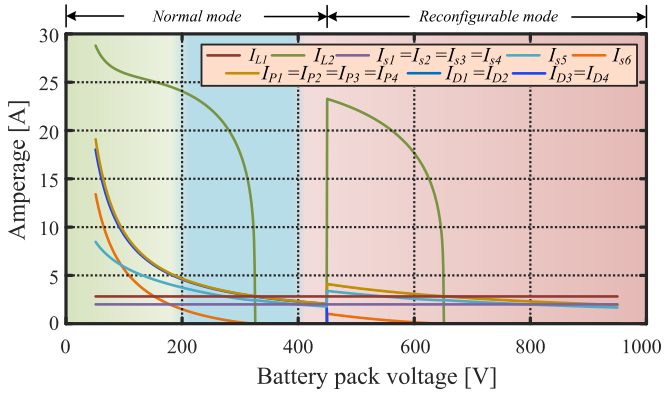

Fig. 6. Amperage of the components under a wide voltage range operation.

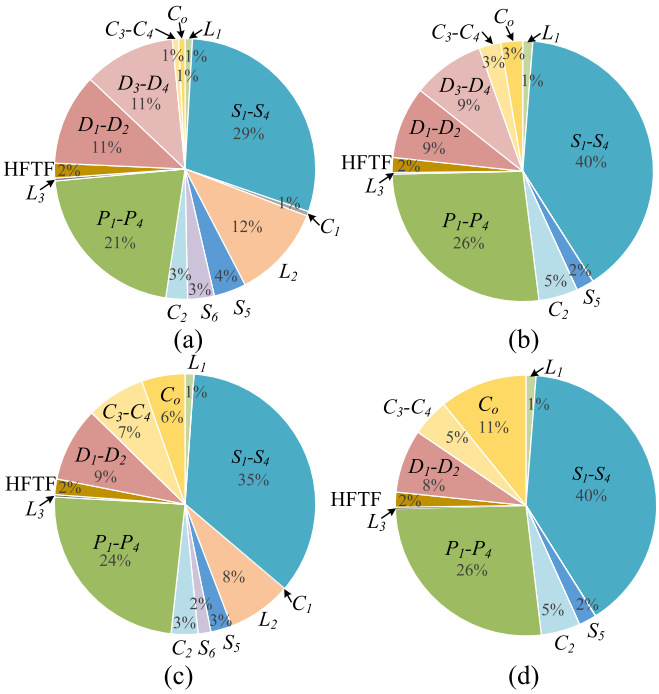

Fig. 7. Loss distribution of the proposed charger at a wide range of battery pack voltages. (a) 250 V. (b) 400 V. (c) 600 V. (d) 800 V.

current stress on the components using the proposed charger's steady-state analytical model, and their results are depicted in Fig. 6. The loss distribution among the devices over a wide range of battery pack voltages is estimated and illustrated in Fig. 7. For better evaluation of the proposed charger, charge cycle efficiency (η_{cycle}) is evaluated, which can be given as follows [12]:

$$\eta_{\text{cycle}} = \int_0^{T_{\text{cc}}} \eta(t)dt + \int_{T_{\text{cc}}}^{T_{\text{cv}}} \eta(t)dt \tag{3}$$

where T_{cc}, T_{cv}, and $\eta(t)$ are the time duration of the CC charging, ending time of CV charging, and instantaneous charger efficiency, respectively. The charge cycle efficiency of the proposed charger at a wide voltage range with a CC–CV charging is evaluated, as depicted in Fig. 8. It is noticed that the proposed charger operates with a cycle efficiency of 95.73% and 95.89% at 400 and 800 V charging, respectively.

A similar analysis is performed and compared with the conventional battery charger under a wide range of battery pack voltages, as illustrated in Fig. 9. The conventional battery charger

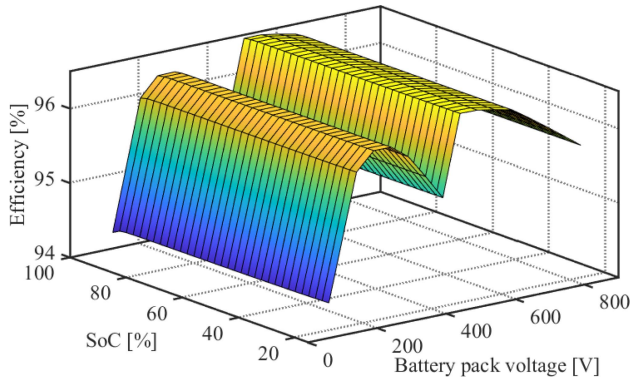

Fig. 8. Efficiency of the proposed charger over a wide range of battery pack voltage and state of charge (SoC).

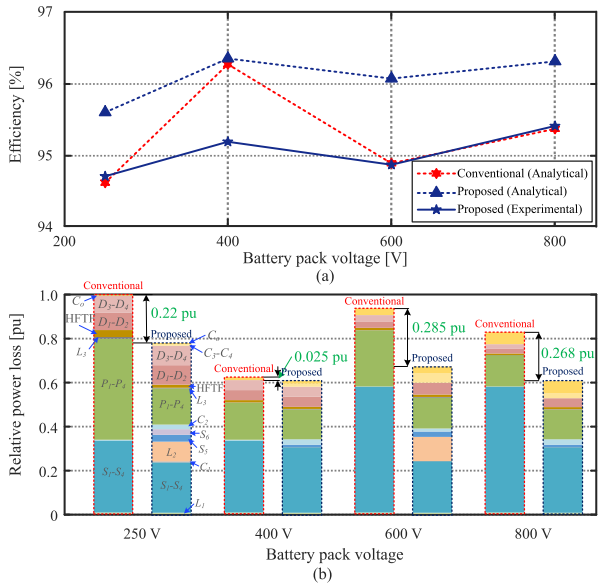

Fig. 9. Performance analysis of the conventional and proposed charger over a wide range of battery pack voltage. (a) Efficiency. (b) Relative power loss distribution among the components.

TABLE II
SPECIFICATIONS AND COMPONENT VALUES OF THE CHARGER

Battery pack voltage [V]	Power factor		Input current THD [%]	
	Conventional	Proposed	Conventional	Proposed
120	0.9967	0.9979	4.87	4.89
250	0.9971	0.9956	4.75	4.06
400	0.9974	0.9979	4.21	3.72
600	0.9985	0.9961	3.05	4.93
800	0.9988	0.9969	3.11	4.47

is realized with a totem-pole PFC followed by a PSFB converter. The efficiency of the conventional and proposed charger is depicted in Fig. 9(a). In addition, conventional and proposed charger losses are assessed from the charger's steady-state models and expressed in per unit (p.u.) as shown in Fig. 9(b). The power loss ($\approx$ 56.8 W) at 250-V battery pack charging of a conventional battery charger is considered as a base value, and the rest of the power losses are graded in p.u. accordingly. It is remarked that the proposed charger can operate at 96.35% peak efficiency with an average efficiency of 96%, which is approximately 1% higher than the conventional battery charger

TABLE III
COMPARISON OF THE PROPOSED RECONFIGURABLE CHARGER WITH EXISTING RECONFIGURABLE BATTERY CHARGERS

	Ref. [5]	Ref. [6]	Ref. [7]	Ref. [8]	Ref. [9]	Ref. [10]	Proposed charger
Configuration	–	Dc–dc	Ac–dc	Ac–dc	Ac–dc	Dc–dc	Ac–dc
Input supply	–	400 V, dc	1-ϕ	1-ϕ	1-ϕ	640–840 V, dc	1-ϕ, 85 – 265 V, 50/60 $\pm$ 1%
Reconfiguration technique	Battery with charge balance circuits	Reconfigurable battery selection circuit	Cascaded secondary rectifiers	Cascaded dual-active bridge and series resonant converter	Tap changing HFTF	Cascaded secondary rectifiers	Reconfigurable secondary rectifier
Auxiliary devices	Reconfigurable battery pack, and BMS	Battery selection circuit	3-winding TF full-bridge rectifier, and switches	3-winding TF, full bridge rectifier, and switches	Tap changing TF and switch	3-winding TF, full-bridge rectifier, and 3 IGBTs	Filter capacitor branch and relay
Charging cord size reduction	×	✓	✓	✓	✓	✓	✓
Component count	High	Medium	High	Medium	Low	High	Low
Device utilization factor	Low	Medium	Medium	High	Medium	Medium	High
Design complexity	High	Medium	Low	Medium	Medium	Medium	Low
Output voltage range [V]	–	400–800	–	400/800	–	250–1000	120–900
Output voltage ripple	No change	Reduces in LV charging	No change	Reduces in LV charging	No change	No change	Reduces in LV charging

over a wide battery pack voltage range. Also, analysis is conducted in terms of the distortion power factor (PF) and input current total harmonic distortion (THD) over wide battery pack voltages, which are listed in Table II. It is noticed that the conventional and the proposed charger operate approximately at unity PF over a wide range of battery pack voltage while maintaining the current THD standards at the grid side. However, conventional battery charger performance is degraded with a change in battery pack voltage. On the other hand, the proposed battery charger has negligible performance degradation over a wide range of battery pack voltage. Overall, the proposed reconfigurable charger operates over a wide output voltage range with greater efficiency, UPF, and maintains the input current THD within IEEE 519:2014 standards. The distinguishing features of the proposed reconfigurable charger in comparison with the existing chargers are summarized in Table III.

IV. CONCLUSION

This letter proposes a new reconfigurable battery charger with a wide output voltage of 120–900 V to charge LV–MV–HV battery EVs with the same power rating. The proposed charger's operating mode selection and control architectures are presented in detail. The proposed topology draws continuous input current due to the boost–buck configuration at the grid side, and it can be reconfigured using a filter capacitor branch and relay on the battery side with a reduced voltage ripple. Detailed simulations and experiments were carried out on a 1.3-kW SiC-MOSFET-based laboratory prototype to assess the proposed charger's viability and its control. The results demonstrate that the proposed reconfigurable charger and the controller maintained the desired dc voltage with allowable ripple and extracted ripple-free sinusoidal current by preserving UPF regardless of the battery pack voltages. The charger operates with cycle efficiencies of 95.73% and 95.89% and THDs of 3.72% and 4.47% at 400 and 800 V, respectively. Therefore, the proposed reconfigurable battery charger is best suited for universal EV charging applications.

REFERENCES

[1] "EV Specifications," USA. Apr. 1, 2023. [Online]. Available: https://www.evspecifications.com/

[2] S. Rivera et al., "Charging infrastructure and grid integration for electromobility," *Proc. IEEE*, vol. 111, no. 4, pp. 371–396, Apr. 2023.

[3] I. Aghabali, J. Bauman, P. J. Kollmeyer, Y. Wang, B. Bilgin, and A. Emadi, "800-V electric vehicle powertrains: Review and analysis of benefits, challenges, and future trends," *IEEE Trans. Transport. Electrific.*, vol. 7, no. 3, pp. 927–948, Sep. 2021.

[4] C. Jung, "Power up with 800-V systems: The benefits of upgrading voltage power for battery-electric passenger vehicles," *IEEE Ind. Electron. Mag.*, vol. 5, no. 1, pp. 53–58, Mar. 2017.

[5] M. Momayyezan, B. Hredzak, and V. G. Agelidis, "Integrated reconfigurable converter topology for high-voltage battery systems," *IEEE Trans. Power Electron.*, vol. 31, no. 3, pp. 1968–1979, Mar. 2016.

[6] J. Y. Kim, B. S. Lee, D. H. Kwon, D. W. Lee, and J. K. Kim, "Low voltage charging technique for electric vehicles with 800 V battery," *IEEE Trans. Ind. Electron.*, vol. 69, no. 8, pp. 7890–7896, Aug. 2022.

[7] A. Khaligh and Y. Tang, "Integrated dual-output grid-to-vehicle (G2V) and vehicle-to-grid (V2G) onboard charger for plug-in electric vehicles," U.S. Patent US10696182B2, Apr. 1, 2023. [Online]. Available: https://patentimages.storage.googleapis.com/f3/ba/16/16b61601723b8e/US10696182.pdf

[8] H. Sarnago, Ó. Lucía, R. Jiménez, and P. Gaona, "Differential-power-processing on-board-charger for 400/800-V battery architectures using 650-V super junction MOSFETS," in *Proc. IEEE Appl. Power Electron. Conf. And Expo.*, 2021, pp. 564–568.

[9] L. N. Sunkara et al., "Optimizing the topology of electrical powertrain for electrical and plug-in hybrid vehicles," India Patent 201811047973, Accessed: Apr. 1, 2023. [Online]. Available: http://ipindia.gov.in/writereaddata/Portal/IPOJournal/1_4879_1.pdf/Part-1.pdf

[10] D. Lyu, T. B. Soeiro, and P. Bauer, "Design and implementation of a reconfigurable phase shift full-bridge converter for wide voltage range EV charging application," *IEEE Trans. Transport. Electrific.*, vol. 9, no. 1, pp. 1200–1214, Mar. 2023.

[11] "Phase-shifted full bridge DC/DC power converter design guide," *Texas Instruments*, Dallas, TX, USA. Accessed: Apr. 1, 2023. [Online]. Available: https://www.ti.com/lit/pdf/tidu248

[12] D. Lyu, T. B. Soeiro, and P. Bauer, "Impacts of different charging strategies on the electric vehicle battery charger circuit using phase-shift full-bridge converter," in *Proc. IEEE 19th Int. Power Electron. Motion Control Conf.*, 2021, pp. 256–263.

[13] D. S. Gautam, F. Musavi, M. Edington, W. Eberle, and W. G. Dunford, "An automotive onboard 3.3-kW battery charger for PHEV application," *IEEE Trans. Veh. Technol.*, vol. 61, no. 8, pp. 3466–3474, Oct. 2012.